Vertical Eddy Mixing in the Tropical Upper Ocean: Its Influence on Zonal Currents

ZUOJUN YU

Joint Center for Earth System Science, Department of Meteorology, University of Maryland at College Park, College Park, Maryland

PAUL S. SCHOPF*

Coupled Climate Dynamics Group, NASA/Goddard Space Flight Center, Greenbelt, Maryland

(Manuscript received 23 August 1996, in final form 29 January 1997)

ABSTRACT

In this study, the authors explore how vertical-mixing parameterizations influence the structure of zonal currents in the eastern equatorial Pacific using an isopycnal ocean model that contains an explicit surface mixed layer. The mixing parameterizations considered are the schemes that depend on the Richardson number (Ri). One of the schemes (the Step scheme) consists of high (ν_c) and low (ν_b) values of mixing coefficients, depending on whether Ri is less than or greater than a critical value. In simulations using the Step scheme, there is a region of large vertical shear just beneath the mixed layer where Ri is low and the mixing coefficient is ν_c; this high mixing controls the depth and strength of the westward surface drift. Near the undercurrent core, Ri is high and the mixing coefficient is ν_b; this low mixing is nevertheless dynamically important in that it affects the strength of the undercurrent. For the Ri-dependent schemes investigated, it is demonstrated that the extrema attained by mixing coefficients at low and high Ri are the crucial factor rather than the detailed structure of the Ri-dependent functions.

1. Introduction

The role of turbulent mixing in the ocean, particularly the tropical upper ocean, has received substantial attention in the past two decades. This is due in no small part to its influence on the equatorial undercurrent and on the surface heat balance. At the time of the NATO Advanced Study Institute on Modelling and Prediction of the Upper Layers of the Ocean (Kraus 1977), mixed layer modeling was being actively pursued as a means to represent the high levels of turbulence found at the ocean's surface (Niiler and Kraus 1977). A problem arose in implementing such models in a wider context because the ocean general circulation models (OGCMs) of the day were based on a fixed vertical discretization that does not lend itself to embedding such a mixed layer model. Other means to simulate the high surface mixing were therefore sought.

Turbulence closure modeling for the ocean mixing was under development at the time (Mellor and Durbin 1975), based on similar work done for the atmosphere (Mellor and Yamada 1974). Development of the ''level 2.5'' turbulence closure model for the ocean was made by Mellor and Yamada (1982) and implemented in a global OGCM by Rosati and Miyakoda (1988).

For the simplest mixing parameterization, eddy coefficients are determined by a *single* parameter that represents the mean ocean state. The suitable parameter for the tropical ocean is the bulk Richardson number (Ri), because of the large mean shear associated with the equatorial undercurrent. Based on empirical studies of Robinson (1966) and Jones (1973), Pacanowski and Philander (1981) proposed a formulation that depends on Ri and remains popular with modelers of tropical circulation.

Using profiles of currents, density, and microstructure taken during Tropic Heat I experiment, Peters et al. (1988) obtained a parameterization that related eddy coefficients to the *mean* Ri from the 4½-day time series. Note that their parameterization was based on the averaged data, instead of the hourly data with fine vertical resolutions that numerical models of general circulations are unable to handle. They found that the dependence of mixing coefficients on the mean Ri is much steeper than that proposed by Pacanowski and Philander (1981) at low Ri (Fig. 1). However, the general character of the two schemes is similar; that is, high mixing is associated with low Ri and low mixing with high Ri.

A recent trend toward layered ocean models (Bleck and Boudra 1986; Gent and Cane 1988; Oberhuber 1993; Murtugudde et al. 1995; Schopf and Loughe 1995), which readily accept the inclusion of a surface mixed layer, has facilitated reexamination of diapycnal mixing in the ocean.

* Current: Institute for Computational Sciences and Informatics, George Mason University, Fairfax, Virginia.

Corresponding author address: Dr. Zuojun Yu, NOAA/PMEL/OCRD, 7600 Sand Point Way, NE, Seattle, WA 98115.
E-mail: zuojun@pmel.noaa.gov

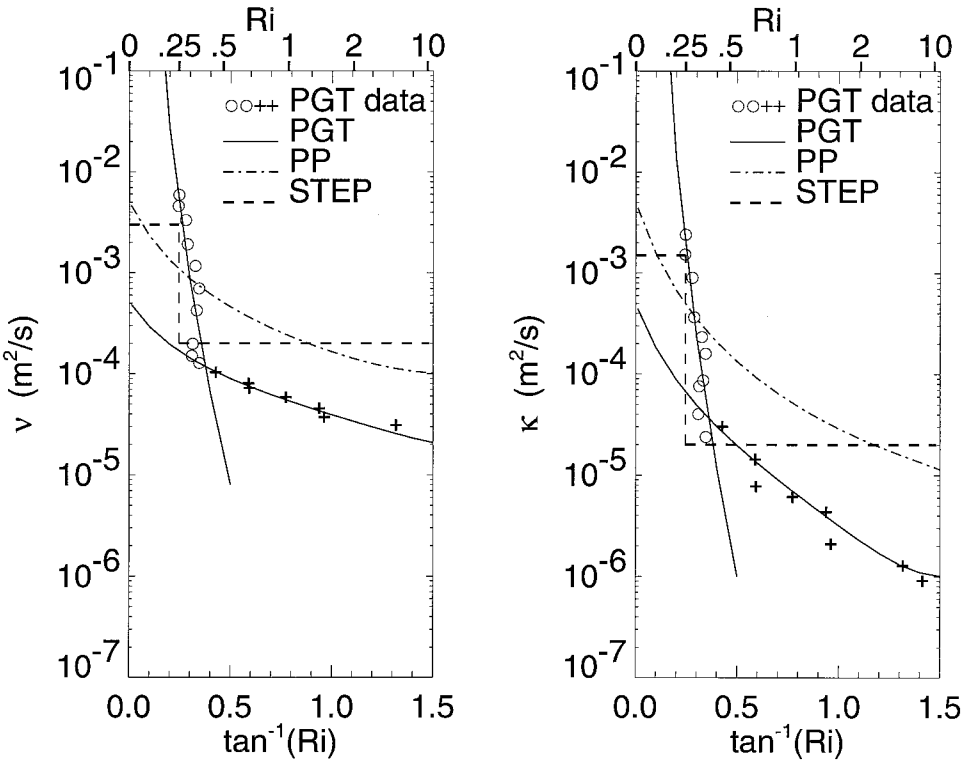

FIG. 1. Mixing coefficients as a function of Richardson number. The Peters et al. (1988) results are based on microstructure measurements at 0°, 140°W: circles are for observations at depth shallower than 81 m, pluses are between 81 and 138 m. Various mixing parameterizations are shown with lines: solid curves are from Peters et al. (1988); dash–dotted curves are from Pacanowski and Philander (1981); and dashed lines are from the Step scheme with its default values.

In isopycnal versions of these models, diapycnal mixing is removed from the numerics and arises as an explicit parameterization—all horizontal mixing is isopycnal, whether through explicit diffusion operators or through implicit diffusion associated with numerics. Chen et al. (1994) proposed a ''hybrid'' mixing scheme, which is a combination of the Kraus and Turner (1967) and Price et al. (1986) models. Below the Kraus–Turner type of surface mixed layer, their tropical OGCM allows mixing to happen only when Ri falls below a critical value Ri_c. This is in keeping with classical studies of shear generated turbulence and mixing (Miles 1961; Howard 1961; Hazel 1972; Thorpe 1973) and recent field-experiments results from Tropic Heat I (Peters et al. 1988; Moum et al. 1989), indicating a highly episodic nature of mixing and a strong dependence on Ri_c. According to the Taylor–Goldstein equation, $Ri_c = 0.25$ (Miles 1961). Observations, however, suggested that Ri_c may be larger or smaller than the theoretical value of 0.25 (e.g., Moum et al. 1989).

The reason for parameterizing turbulence in terms of Ri in strong mean shear regions is pragmatic because OGCMs are limited by their temporal and vertical resolutions to simulate the turbulence process itself. Schemes such as Pacanowski and Philander's essentially separate *two regimes* of ocean mixing—a low-Ri (high mixing) regime from a high-Ri (low mixing) regime (see, e.g., Smith and Hess 1993). We therefore propose a simpler scheme that embodies this character: our Step scheme chooses an explicit high mixing value when Ri is low and keeps a small background mixing for large Ri. This allows for a more direct comparison with the earlier Ri-dependent schemes and for demonstration of parameter sensitivity in a clearer fashion.

Questions that we consider include the following. How do parameters in these schemes determine the vertical structure of upper-ocean currents? Is there anything in the shape of the Ri dependence beyond the essential physics of high and low mixing regimes? Does the dependence of mixing coefficients on Ri introduce any substantially new physics from the older concept of a turbulent surface mixed layer?

2. Model description and methodology

The model is a 14½-layer, quasi-isopycnal OGCM of the tropical Pacific, which is modified from Schopf and Loughe (1995) to include salinity effects and more layers for better resolution in the uppermost part of the water column. The topmost layer is treated as a bulk turbulent mixed layer, with its dynamics essentially being those in Niiler and Kraus (1977). It includes mixing effects due to wind stirring, penetrating radiation, and

surface cooling. A shallowing mixed layer is dealt with by relaxing back to the Monin–Obukhov depth.

a. Vertical mixing schemes

Below the surface mixed layer, vertical eddy mixing is assumed to depend on Ri, which is calculated at each layer interface. Four different mixing schemes are contrasted. Most of them require specification of both viscosity (ν) and diffusivity (κ), and κ is used to mix both temperature and salinity fields.

PP scheme: For computational convenience, we have approximated the Pacanowski and Philander (1981) scheme as

$$\nu = \frac{50 \times 10^{-4}}{(1 + 5\text{Ri})^2} + 10^{-4}\ \text{m}^2\ \text{s}^{-1}, \tag{1}$$

$$\kappa = \frac{50 \times 10^{-4}}{(1 + 5\text{Ri})^3} + 10^{-5}\ \text{m}^2\ \text{s}^{-1}, \tag{2}$$

where $\text{Ri} = N^2/U_z^2$, N is the local Väisälä frequency, and U_z is vertical current shear.

PGT scheme: Neglecting the uncertainty in the parameterization proposed by Peters et al. (1988), we will use

$$\nu = 5.6 \times 10^{-8}\ \text{Ri}^{-8.2} + \frac{5 \times 10^{-4}}{(1 + 5\text{Ri})^{1.5}} + 2 \times 10^{-5}\ \text{m}^2\ \text{s}^{-1}, \tag{3}$$

$$\kappa = 3 \times 10^{-9}\ \text{Ri}^{-9.6} + \frac{5 \times 10^{-4}}{(1 + 5\text{Ri})^{2.5}} + 10^{-6}\ \text{m}^2\ \text{s}^{-1}. \tag{4}$$

Note that in this scheme mixing goes to infinity as Ri approaches zero.

CRB scheme: In the Chen et al. (1994) scheme, Ri is compared with $\text{Ri}_c = 0.25$ at a fixed time interval. If $\text{Ri} < \text{Ri}_c$ between two neighboring layers, k and $(k + 1)$, then the velocities and buoyancies in these two layers are partially mixed according to

$$F_k' = F_k - \left(1 - \alpha\frac{\text{Ri}}{\text{Ri}_c}\right)(F_k - F_{k+1})\frac{h_{k+1}}{(h_k + h_{k+1})}, \tag{5}$$

$$F_{k+1}' = F_{k+1} + \left(1 - \alpha\frac{\text{Ri}}{\text{Ri}_c}\right)(F_k - F_{k+1})\frac{h_{k+1}}{(h_k + h_{k+1})}, \tag{6}$$

where F denotes the variable to be mixed, F' is the same variable after mixing, and h is the layer thickness. The coefficient α is set to unity at $k = 1$, and is 0.55 (for velocities) or 0.1 (for buoyancies) at all other interfaces. Equations (5) and (6) were designed so that Ri generally increases to Ri_c after two passes through the water column.

Step scheme: Based on the argument of *two mixing regimes*, we propose a simple scheme as follows:

$$\nu = \begin{cases} \nu_c, & \text{for Ri} < \text{Ri}_c \\ \nu_b, & \text{for Ri} \geq \text{Ri}_c; \end{cases} \tag{7}$$

$$\kappa = \begin{cases} \kappa_c, & \text{for Ri} < \text{Ri}_c \\ \kappa_b, & \text{for Ri} \geq \text{Ri}_c, \end{cases} \tag{8}$$

where ν_c, ν_b, κ_c, κ_b, and Ri_c are all tuneable constants. In this study, we assume Prandtl number (ν/κ) to be 2 and 10 for low and high Ri, respectively, which is consistent with Peters et al. (1988). The default values used for viscosity are $\nu_c = 30 \times 10^{-4}\ \text{m}^2\ \text{s}^{-1}$ and $\nu_b = 2 \times 10^{-4}\ \text{m}^2\ \text{s}^{-1}$; therefore, default values for diffusivity are $\kappa_c = 15 \times 10^{-4}\ \text{m}^2\ \text{s}^{-1}$ and $\kappa_b = 2 \times 10^{-5}\ \text{m}^2\ \text{s}^{-1}$. The default value for Ri_c is 0.25.

b. Other mixing in the model

Additional vertical mixing occurs whenever the water column becomes statically unstable, in which case explicit convective adjustment is applied to the temperature and salinity fields. The horizontal smoothing necessary to keep the model numerically stable is provided by a modified Shapiro (1970) filter. For the experiments reported in this paper, we used eighth-order filters on velocity fields and fourth-order ones on temperature and salinity fields, applying each filter once a day. We wish to note that model output is generally sensitive to horizontal smoothing used in momentum equations, which itself is a separate research topic.

c. Model basin, spinup, and output

The model basin extends zonally from 120°E to 80°W and meridionally from 40°S to 40°N. The eastern and western boundaries resemble the real coastlines of the Pacific Ocean, whereas artificial walls are placed at 40°S and 40°N. The horizontal resolution is 1.25° longitudinally and 0.67° latitudinally. The 14 layers are spread over roughly the upper 3000 m of the water column with at least 8 layers covering the top 300 m in the equatorial region.

The wind stress is a modified version of the Hellerman and Rosenstein (1983) climatology. Harrison (1989) pointed out that these estimates are too high in the Tropics, so the values used in this study have been reduced by 20%. The wind data is on a 2° × 2° grid, and is interpolated onto the OGCM's finer grid. The surface freshwater and heat fluxes are based on relaxation back to observed sea surface salinity (Levitus 1982) and sea surface temperature (Reynolds 1982) fields, as in Haney (1971). The surface salinity is restored to the climatological, monthly mean values on the ocean-model grid with a relaxation time scale of one month. The surface heat flux is evaluated on two grids: strong damping to the climatological, monthly mean SST is done on a coarse 5° × 4° grid, with weaker damping imposed on the ocean-model grid; in this way, model SST is constructed to resemble the observations quite closely, while still allowing small-scale temperature structures to

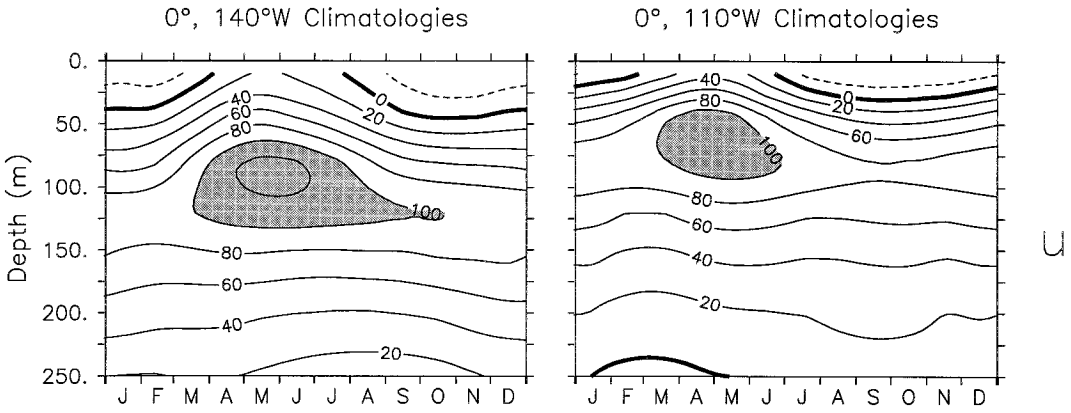

FIG. 2. Seasonal cycles of equatorial zonal currents from observations taken at 140°W and 110°W. Contour intervals are 20 cm s^{-1}, dashed lines indicate westward flows, and shaded regions highlight the undercurrent core. The undercurrent is strongest in the spring; the surface zonal flow is eastward during the spring and westward at other times. After McPhaden and McCarty (1992).

develop (see section 3b of Schopf and Loughe 1995 for details).

The base experiment was run using the Pacanowski and Philander (1981) scheme, in which the initial temperature and salinity fields are taken from the Levitus (1982) climatology and the initial velocity field is a state of rest. It is integrated for 4 years. For the remainder of the experiments, the initial conditions are taken from the end of the second year of the base experiment; the model is integrated for another 2 years with specific changes in the mixing parameterization, and results from the last year are used for comparisions.

3. Results

This study focuses on the eastern, equatorial Pacific Ocean, which shows a distinct annual cycle in zonal currents characterized by an eastward momentum increase during springtime (Fig. 2). The Tropical Oceans Global Atmosphere current meter mooring at 0°, 140°W is used for the key model/data comparison, because it has a long observational history and because it was also the location of Tropic Heat I (Peters et al. 1988); additional comparisons will be made at 0°, 110°W, another mooring site with a long data record. At 140°W, the surface flow is westward (the South Equatorial Current) from August through March with a maximum speed slightly over 20 cm s^{-1}; the current becomes eastward below a depth of about 40 m (the Equatorial Undercurrent) with a maximum speed somewhat weaker than 100 cm s^{-1} and centering around 125 m. From April to July, the surface current becomes eastward, the undercurrent intensifies to over 120 cm s^{-1}, and its core rises to about 85 m. Similar features exist at 110°W, except that the westward drift and the undercurrent core are shallower, and the maximum core speed is weaker.

a. Model simulations using various mixing schemes

At 0°, 140°W simulations using all four mixing schemes show an increase of eastward momentum from April through June, as well as a shallowing undercurrent core from about 125 m in January to about 90 m in May (Fig. 3). However, the model undercurrents produced using the Step, PP, and PGT schemes are about 20%–30% stronger than what is observed (left panel of Fig. 2), and that with the CRB scheme is about 50% stronger. With the Step and PP schemes (upper panels), the depth of the westward surface drift and its annual cycle are similar to the observations, but the PGT and CRB schemes (lower panels) produce a westward drift that is too deep to be realistic.

Figure 4 shows values of Ri sampled every 3 days near 0°, 140°W (the exact grid point is not at 0°, 140°W, so we use the nearest points) from each of the above experiments, as well as the averaged Ri from the observations obtained by Peters et al. (1988). Above the undercurrent core, Ri is generally low in all four cases. There is a peculiarity in the case with the PGT scheme that very high Ri (Ri $>$ 2) appears at the base of the second layer (near 60 m) episodically. This is probably due to the high level of mixing allowed by the scheme, which can homogenize adjacent layers. Because the model uses a staggered horizontal grid, the evaluation of current shear is not done at exactly the same locations as the evaluation of the static stability, and the averaging process in the presence of such strong stabilization leads to situations where the current is well mixed but a slight jump occurs in the density.

Since the depth of the undercurrent core is well simulated in all experiments (Fig. 3), it is not surprising that Ri becomes large at about the same depth as the observations. What is troublesome, however, is the tendency of the model to produce high Ri below the core of the undercurrent in all cases, in contrast with the microstructure

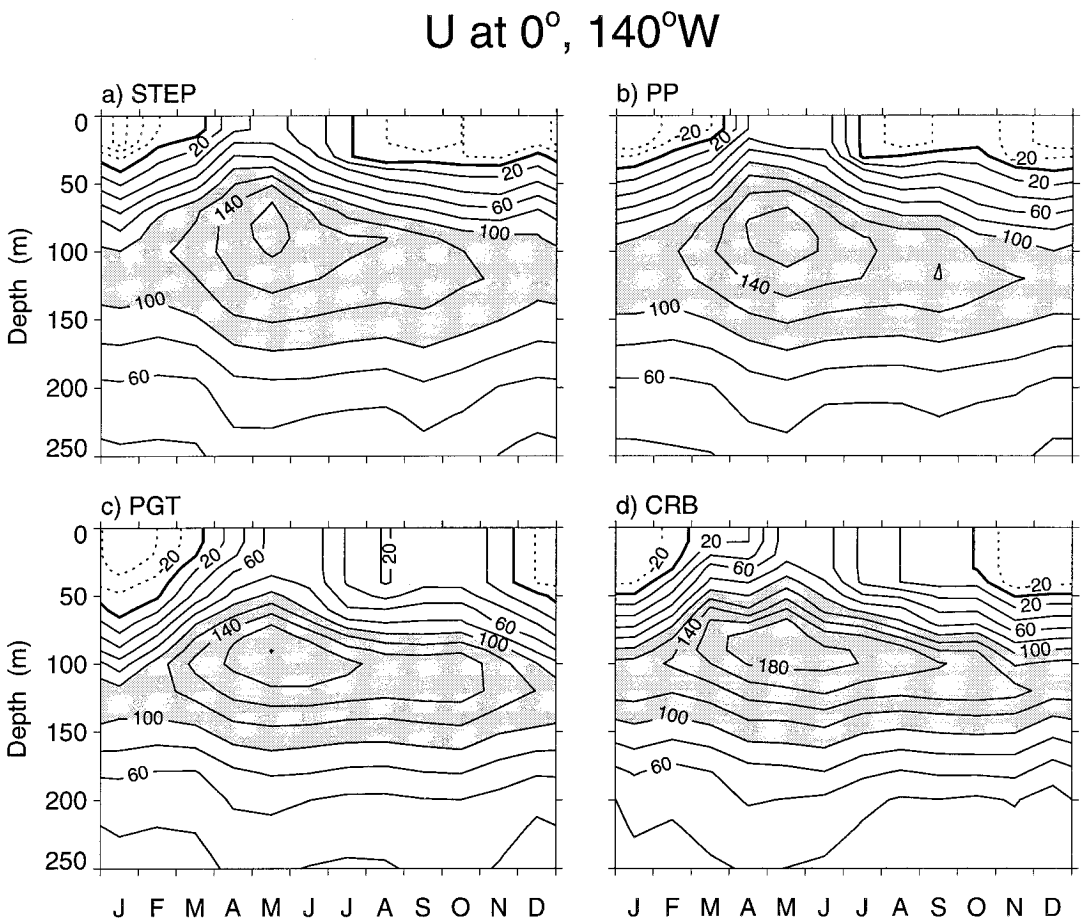

FIG. 3. Seasonal cycles of equatorial zonal currents at 140°W from model simulations using mixing schemes proposed by Pacanowski and Philander (1981, upper-right panel), Peters et al. (1988, lower-left panel), and Chen et al. (1994, lower-right panel), as well as our Step scheme with its default values (upper-left panel). Monthly mean values from the last year of each experiment are used. Contour intervals are 20 cm s^{-1}, dashed lines indicate westward flows, and shaded regions indicate speed greater than 100 cm s^{-1}.

measurement (solid curves in Fig. 4). This discrepency may in part be due to the model's coarse vertical resolution there, which is 70 m or larger for layer 8 as indicated by the dots along the left axis of each panel.

In summary, mixing above the undercurrent core is dominated by low-Ri values, whereas mixing at the core is determined by high-Ri values. Next, we will use the Step scheme to explore the model sensitivity to mixing values at high and low Ri, and to the value of Ri_c.

b. Sensitivity test using the Step scheme

1) SENSITIVITY TO ν_c

Three test experiments were carried out with high mixing coefficient ν_c of 50×10^{-4}, 10×10^{-4}, and 2×10^{-4} m^2 s^{-1}, while keeping the background mixing fixed at $\nu_b = 2 \times 10^{-4}$ m^2 s^{-1}. With a larger value of ν_c, the westward drift penetrates deeper (top panel of Fig. 5), whereas with a smaller ν_c, it is more surface trapped (middle and bottom panels of Fig. 5). The parameter has little effect on the solution near and below 125 m, as might be expected from an examination of Fig. 4.

This model sensitivity helps to explain why the westward surface drift from the PGT and CRB schemes are so deep (lower panels of Fig. 3). In the PGT scheme, there is no upper bound for mixing values as Ri approaches zero; therefore, mixing can attain very large values as Ri drops below Ri_c (unrealistically large because their data showed an averaged maximum of 60×10^{-4} m^2 s^{-1}). For the CRB scheme, mixing happens rapidly when $Ri < Ri_c$, which is equivalent to a very large value of mixing, if not infinity. Therefore, the deep extent of the westward drift produced by both of these schemes results from excessive mixing in the low-Ri regime.

Mixing schemes like Pacanowski and Philander's were originally designed to simulate the effects of a surface mixed layer in models with fixed level coordinates. Since this model already has an explicit turbulent surface mixed layer, is it possible to eliminate the high mixing from the

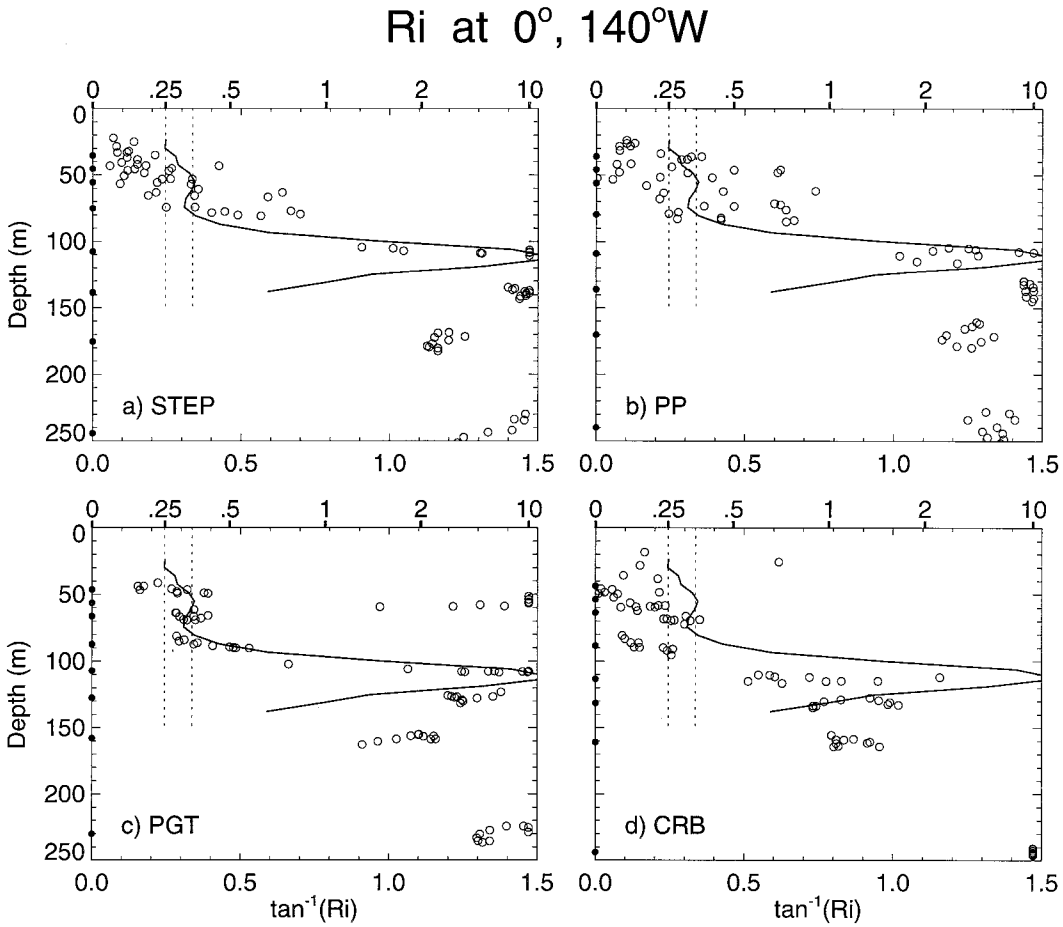

FIG. 4. Values of Richardson number near 0°, 140°W from model simulations during November using the Step (with its default values, upper-left panel), Pacanowski and Philander (1981, upper-right panel), Peters et al. (1988, lower-left panel), and Chen et al. (1994, lower-right panel) schemes. Note that Ri > 10 is plotted along Ri = 10 for model Richardson numbers. Solid curve indicates observed Richardson number obtained by Peters et al. (1988). The small dots along the left axis of each panel indicate the average location of layer interfaces.

Step scheme? The case with $\nu_c = \nu_b = 2 \times 10^{-4}$ m^2 s^{-1} indicates that a significant amount of mixing is required *below* the mixed layer: without this high mixing regime, the model produces a very unrealistic near-surface-flow pattern (bottom panel of Fig. 5). The physics is simple: the equatorial undercurrent leads to shear instability just beneath the mixed layer that results in strong mixing. The importance of shear-induced mixing in the stratified region below the mixed layer was recognized by Large et al. (1994). More discussions on this low-Ri (high mixing) regime will be presented in section 3d.

2) SENSITIVITY TO ν_b

Six additional experiments were conducted with background mixing $\nu_b = 30 \times 10^{-4}$, 4×10^{-4}, 2×10^{-4}, 1×10^{-4}, 0.5×10^{-4}, and 0×10^{-4} m^2 s^{-1}, while keeping ν_c fixed to 30×10^{-4} m^2 s^{-1}. Results are shown in Figs. 6 and 7. The experiment with $\nu_b = 30 \times 10^{-4}$ m^2 s^{-1}, which is essentially that of a constant-coefficient case because $\nu_b = \nu_c$, fails to reproduce the annual cycle, a major distortion of the solution (top panels of Fig. 6). Consistent with the notion that ν_c controls the flow pattern in the near-surface region, the solutions of the other cases are all similar close to the surface. The primary change is associated with the maximum speed of the undercurrent core. The undercurrent maximum at 140°W increases from about 140 to 160 to 180 cm s^{-1} as the mixing is decreased from 4×10^{-4} to 2×10^{-4} to 0×10^{-4} m^2 s^{-1} (left panels of Figs. 6 and 7). The same feature is also seen at 110°W (right panels of Fig. 6).

3) SENSITIVITY TO Ri_c

Three tests were done with $\mathrm{Ri}_c = 0.2$, 0.3, and 0.5, while ν_c and ν_b kept their default values. The speed of the EUC core at both 140°W and 110°W became slightly weaker as Ri_c increased toward 0.5, but otherwise solutions were not sensitive to Ri_c. In fact, the sensitivity to Ri_c depends on vertical resolution. The property that our so-

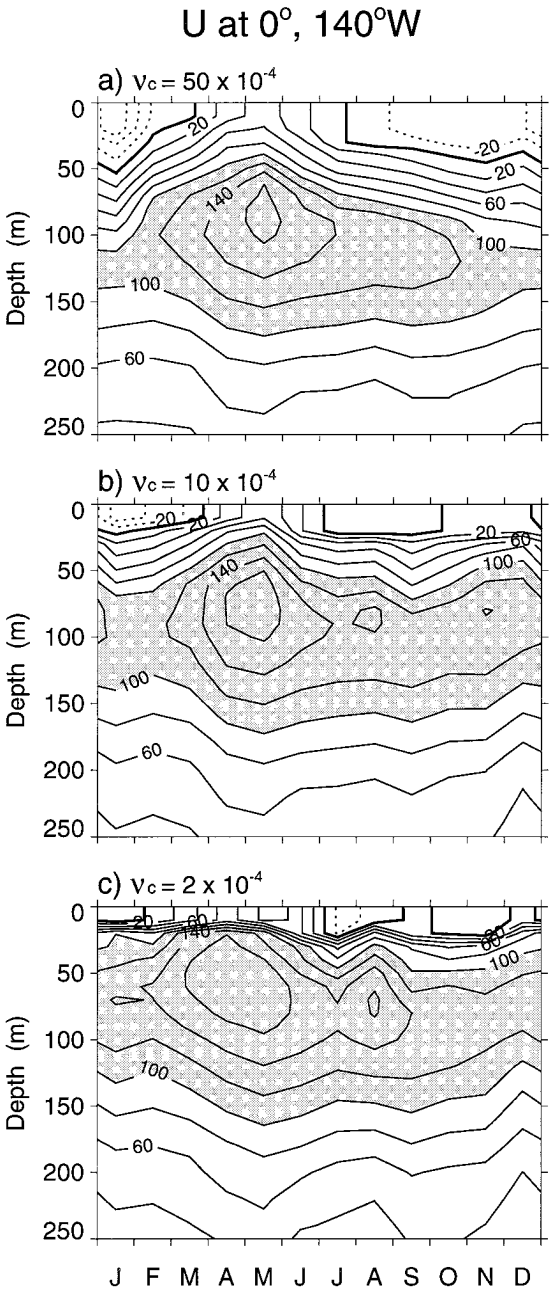

FIG. 5. Similar to Fig. 3 except for model sensitivity study using the Step scheme. All three simulations have the same background mixing $\nu_b = 2 \times 10^{-4}$ m^2 s^{-1}, but different values of ν_c for Ri $<$ Ri$_c$: (a) $\nu_c = 50 \times 10^{-4}$ m^2 s^{-1}, (b) $\nu_c = 10 \times 10^{-4}$ m^2 s^{-1}, and (c) $\nu_c = 2 \times 10^{-4}$ m^2 s^{-1}.

lutions are similar for Ri$_c \leq 0.5$ appears because the resolution for our upper ocean is good. Larger values of Ri$_c$ are required when the model has a coarser vertical resolution (Gent 1991).

c. Mimicking complex schemes using the Step scheme

If the Ri-dependent schemes are to separate *two regimes* of ocean mixing, it should be possible to replicate the results of the PP, PGT, and CRB schemes using the Step scheme by adjusting its two parameters, ν_c and ν_b, appropriately. In addition, because the PGT scheme allows such high mixing for low Ri, which we have seen causes an abnormally deep westward drift (lower-left panel of Fig. 4), we limit the mixing in the PGT scheme to have a maximum value of 30×10^{-4} m^2 s^{-1}, a value consistent with their maximum values for viscosity from the measurement (Fig. 1).

Figure 7 shows the results from the six experiments: left panels show simulations from the Step scheme with different ν_b and right panels show solutions using the PP, PGT (with upper bound), and CRB schemes. Major differences among the simulations are found by moving vertically between panels, that is, when the background mixing ν_b in the Step scheme is changed. Moving horizontally is akin to altering the details of the shape of the Ri-dependent mixing coefficients, but not their extreme values. Similar results are found at 0°, 110°W.

d. Stability in the tropical Pacific Ocean

To gain a better sense of the model behavior, Fig. 8 shows sections along the equator of Ri, the temperature, and the zonal current from the experiment that uses the default values of the Step scheme. We have chosen to plot the monthly mean values for November (the month when Tropic Heat I was conducted) to avoid problems with averaging around the year. The value of Ri is stored every 3 days and averaged along the model interfaces at each longitude. The plotting routine uses this data at the monthly mean position of the layer base, so some distortion is possible in the exact position of each contour, but the essential features are not very different from results plotted from individual snapshots of the simulation. One noticeable feature is that maximum Ri (top panel) follows both the thermocline (middle panel) and the undercurrent core (bottom panel), which explains why the mixing value for high Ri mainly affects the speed of undercurrent core.

A more important feature of the model is that the contour for Ri$_c = 0.25$ (the thin dashed line in the top panel) extends slightly deeper than the surface-mixed-layer depth (indicated by the thick dashed line in the top panel). Figure 9 shows a more detailed picture of this rather thin region where Ri $<$ Ri$_c$. The low-Ri regime generally extends below the surface mixed layer over the central and eastern oceans, thereby allowing vertical mixing to panetrate into the stratified zone below. Meridionally, this low-Ri region is confined within the Tropics: It extends from 3°S to 6°N along 140°W, and even more equatorially trapped toward the east and the date line (not shown).

It is a feature of the equatorial Pacific flow that Ri is driven to low values near the surface in the central and eastern part of the basin through the presence of strong shear in the zonal current: The surface current is westward for much of the year, while the deeper

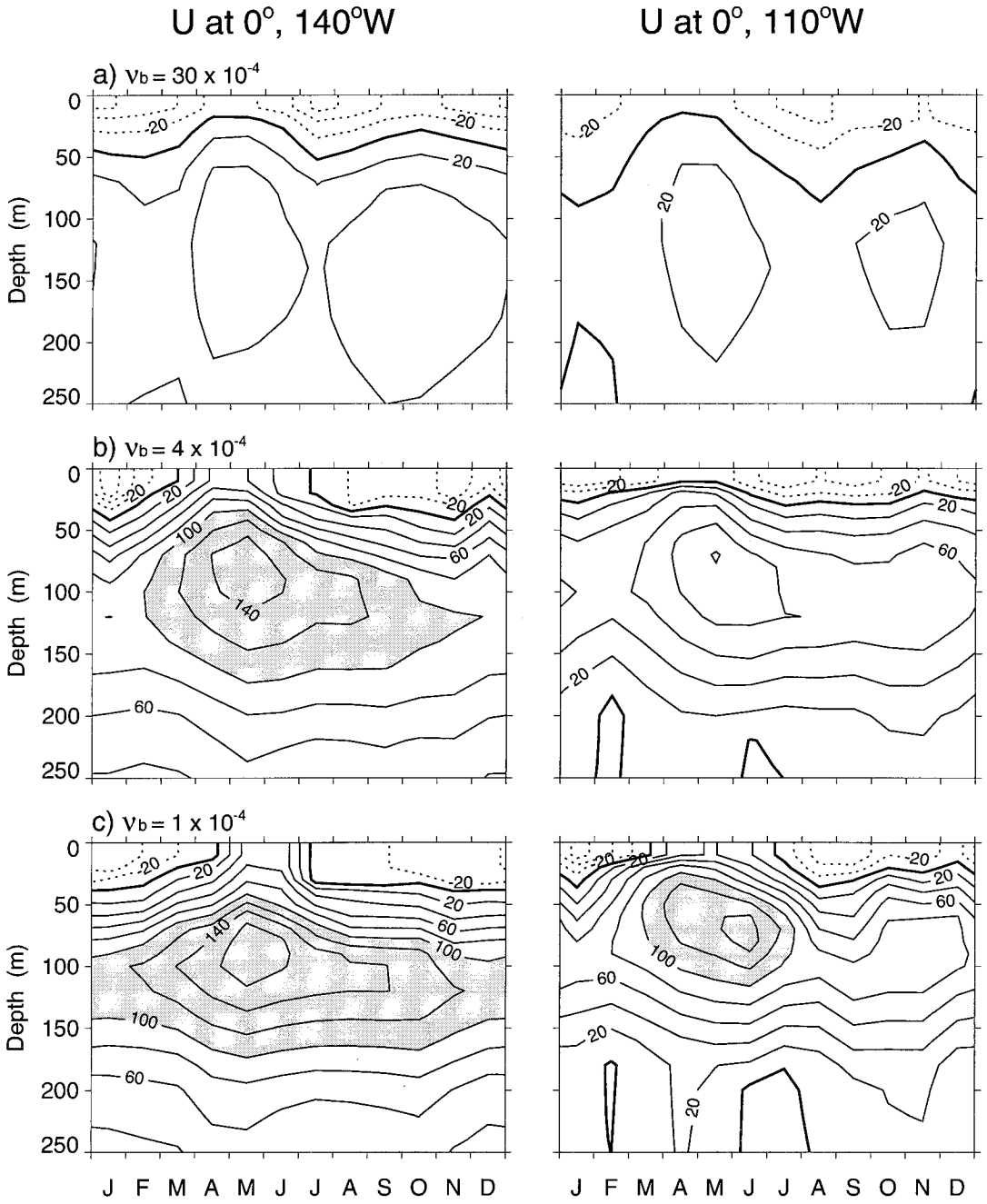

FIG. 6. Similar to Fig. 3 except for model sensitivity study using the Step scheme. All simulations shown here have $\nu_c = 30 \times 10^{-4}$ m^2 s^{-1} for Ri $<$ Ri$_c$, but different values of background mixing: (a) $\nu_b = 30 \times 10^{-4}$ m^2 s^{-1}, (b) $\nu_b = 4 \times 10^{-4}$ m^2 s^{-1}, and (c) $\nu_b = 1 \times 10^{-4}$ m^2 s^{-1}. The left panels are for 0°, 140°W, and the right ones are for 0°, 110°W.

flow is eastward. In the presence of a negative, zonal temperature gradient, the advective tendency for the stability is negative:

$$\frac{\partial}{\partial t}\left(\frac{\partial \rho}{\partial z}\right) = \frac{\partial u}{\partial z}\frac{\partial \rho}{\partial x} + \cdots . \tag{9}$$

In the cold tongue region, the near-surface Ri is therefore decreased by this effect, decreased by the generation of the current shear itself, and increased by the presence of strong surface heating. The bulk mixed layer equations of Kraus and Turner (1967) treat the surface mixing according to a balance of the total kinetic and potential energy,

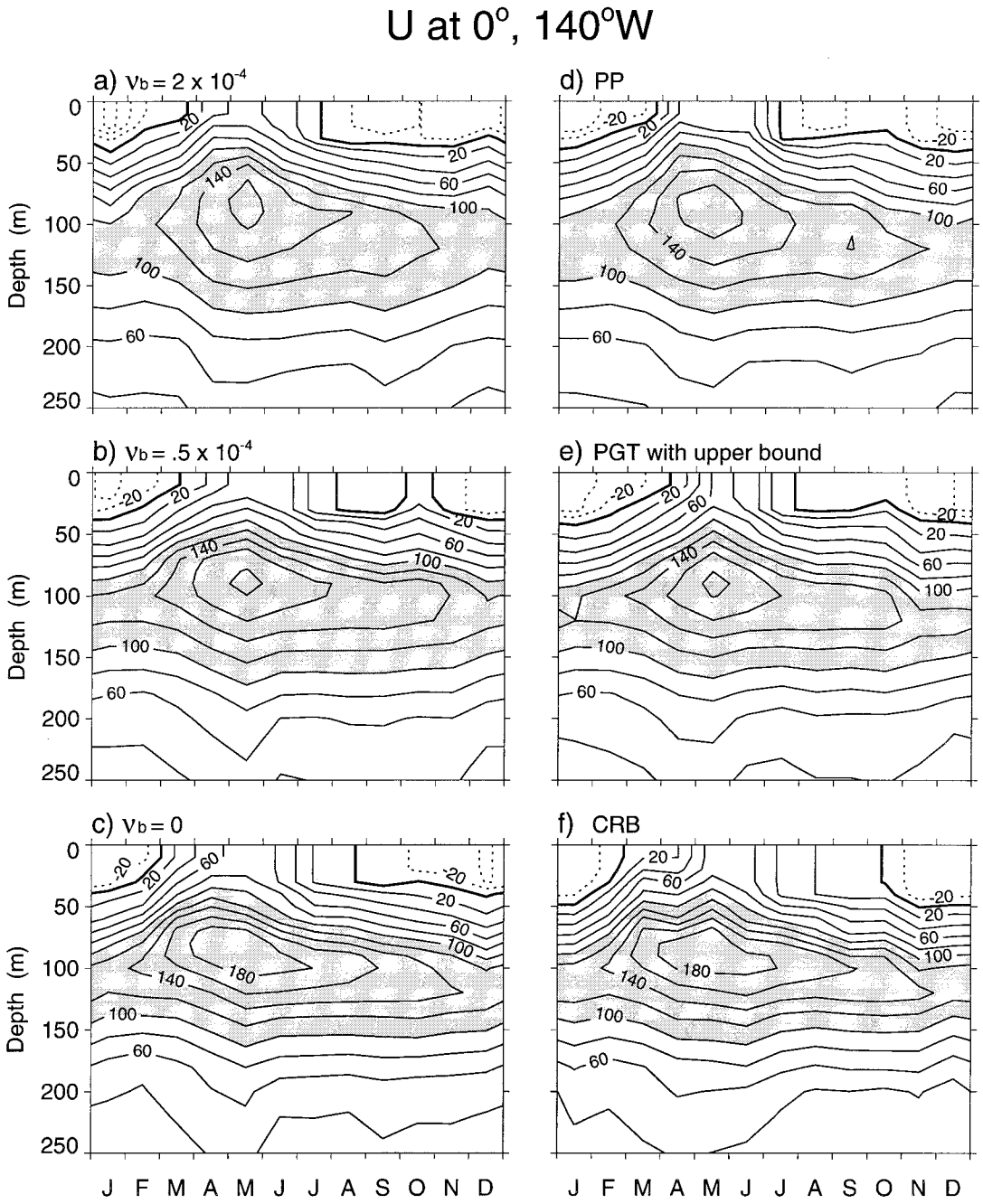

FIG. 7. Comparison of Step scheme with other proposed schemes for zonal current at 0°, 140°W: the simulations in the left panels use the Step scheme with $\nu_c = 30 \times 10^{-4}$ m^2 s^{-1} for Ri $<$ Ri$_c$, but different background mixing: (a) $\nu_b = 2 \times 10^{-4}$ m^2 s^{-1}, (b) $\nu_b = 0.5 \times 10^{-4}$ m^2 s^{-1}, and (c) $\nu_b = 0$; the panels on the right were obtained using (d) Pacanowski and Philander (1981) scheme, (e) Peters et al. (1988) scheme in which mixing is not allowed to exceed 30×10^{-4} m^2 s^{-1}, and (f) Chen et al. (1994) scheme.

and can therefore lead to situations in which Ri is low below the surface mixed layer.

Below this key region, however, Ri in the model remains very high. Note that Ri shown in the top panel of Fig. 8 is contoured in powers of 10 so that the ocean rapidly moves away from a region where mixing varies with Ri to a region with a fixed background value.

4. Discussion and conclusions

This paper emerged out of our efforts to improve model simulations of the near-surface currents in the cold tongue region of the Pacific Ocean. Numerous tuning experiments, in which we altered parameters in the Pacanowski and Philander (1981) and Peters et

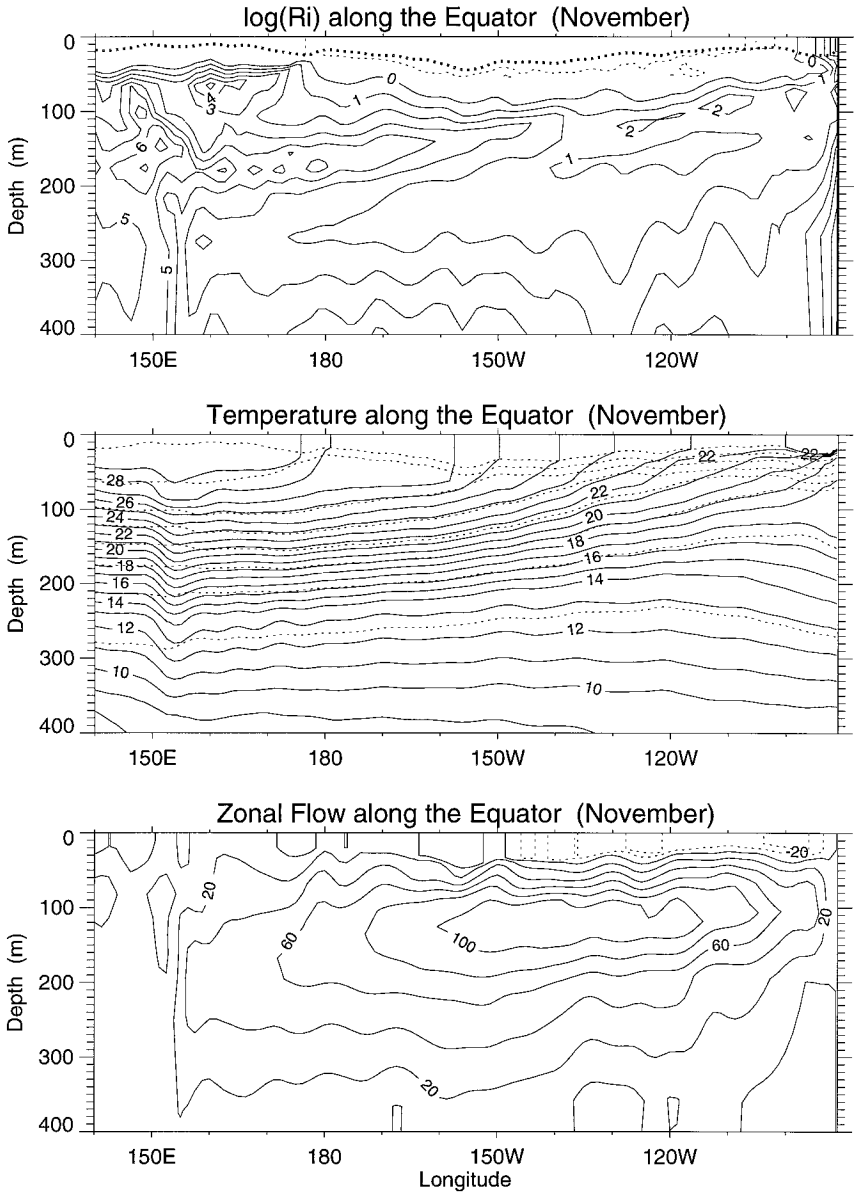

FIG. 8. Sections of log(Ri), temperature, and zonal flow along the equator for November from the Step scheme with its default values. The heavy dashed line in the top panel indicates the surface mixed layer. The thin dashed lines indicate $Ri_c = 0.25$ (top panel), layer interfaces (middle panel), and westward flows (bottom panel). Contour intervals are 1 for positive log(Ri), 1°C for temperature, and 20 cm s^{-1} for zonal flows.

al. (1988) mixing schemes, led to our proposing the Step scheme as a simple parameterization for vertical eddy mixing in the tropical upper ocean. We have found that, consistent with earlier views of turbulence, it is useful to interpret mixing in the tropical ocean as being composed of low-Ri and high-Ri regimes. Thus, the Ri-dependent schemes of Pacanowski and Philander (1981) and Peters et al. (1988) can be understood in terms of *two primary mixing regimes*: a low-Ri (high mixing) regime, which controls the depth and strength of the westward surface drift, and a high-Ri (low mixing) regime, which controls the speed of the undercurrent core.

An essential feature of any mixing scheme for the tropical ocean is how it handles mixing at the extremes of Ri (Figs. 5–7). Use of either the Pacanowski and Philander (1981) or Peters et al. (1988) parameterization should produce similar results under conditions where the mixing coefficients have similar extrema. That the Peters et al. (1988) coefficients go to infinity at Ri = 0 can easily be handled by limiting it to a reasonable value (right-middle panel of Fig. 7). We find no reason to abandon either of

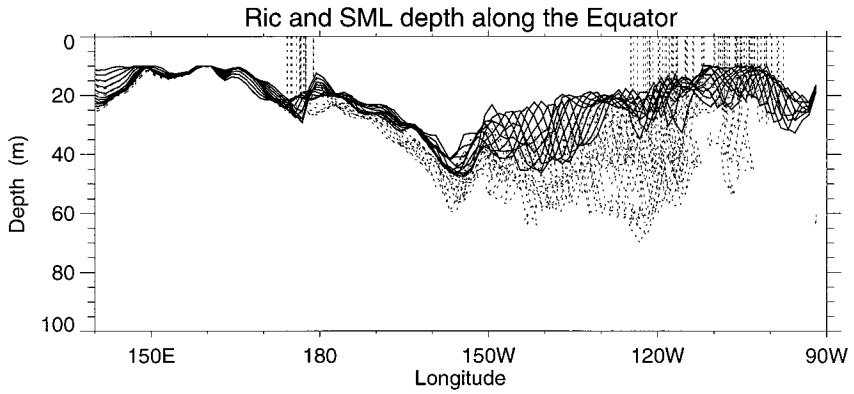

FIG. 9. Distributions along the equator of the critical Richardson number (dashed lines) and surface-mixed-layer (SML) depth (solid lines) during November (sampled every 3 days) using the Step scheme with its default values. It is this near-surface region in between the SML and $Ri_c = 0.25$ contour that has strong influence on the vertical structure of the zonal flow.

these existing schemes in tropical OGCMs, nor any reason to adopt one over the other, or over the Step scheme as proposed here, other than a minor savings in computation and a simplification of the parametric form that helps to understand the model physics.

It remains a concern that the model fails to provide a significantly lowered Ri below the undercurrent core, as suggested by observations (e.g., Peters et al. 1988). This is associated with a thermostad beneath the undercurrent that the model fails to reproduce. Observational evidence (Qiao and Weisberg 1997) suggests that there is significant cross-isopycnal flow in this region, presumably due to diapycnal fluxes. Since the relationship among Ri, mixing coefficient, stability, and shear is highly nonlinear, we had hoped that a suitable shape for the dependence of mixing coefficients on Ri might lead to the formation of such a thermostad. Unfortunately, we find no evidence in the model that there is a preference for thermostad formation for any of the Ri-dependent schemes, which is likely a failure due to the coarse vertical resolution found there in the model (see Fig. 4 and its discussion). We suspect that the dynamics of thermostad formation may also lie outside the realm of diapycnal mixing alone (and may, for example, involve horizontal mixing and vorticity dynamics).

However, not all diapycnal mixing needs to be ascribed to a Ri-based physics when Ri is determined from the *resolved* scales of the numerical model. Parameterizations based on internal wave breaking and other physics have been proposed that may rely on Ri criticality on *small* scales, but that do not involve a requirement for *large* scale shear. Studies of internal wave breaking (Gargett and Holloway 1984; Moum and Osborn 1986) suggest that dissipation (ϵ) in the ocean can be modeled according to

$$\epsilon = aN^{\gamma}, \tag{10}$$

where a and γ are parameters to be determined. Kraus (1990) argued that this leads to a mixing coefficient for buoyancy (K_b) of

$$K_b = \frac{5.75 \times 10^{-8}}{N} \text{ m}^2 \text{ s}^{-1}, \tag{11}$$

(he did not comment on momentum). Equation (11) gives estimates of κ in the range of $0.1 \times 10^{-4} - 1.0 \times 10^{-4}$ m^2 s^{-1}, with the smaller values found in the upper levels of the domain they considered. We have tried to add such effects to the model, but have found no visible impact on the results for the tropical upper-ocean case. Whether we should retain such effects for isopycnal modeling in the global domain is a question outside the scope of this paper.

The turbulence closure methods used in Rosati and Miyakoda (1988) and Blanke and Delecluse (1993) provide an alternative means of computing mixing coefficients. We note that in these models, the mixing coefficient is proportional to the eddy turbulence energy level, which is predicted by the closure model. It is a feature of these models, however, that this energy is largely generated by release of mean shear kinetic energy and is used up in work against bouyancy:

$$\frac{\partial e}{\partial t} = K_m\left(\frac{\partial U}{\partial z}\right)^2 - K_\rho N^2 + K_e\frac{\partial e}{\partial z}, \tag{12}$$

in the notation of Blanke and Delecluse (1993), where e is the eddy kinetic energy and K_m, K_ρ, and K_e are mixing coefficients for momentum, buoyancy, and eddy kinetic energy flux. This is essentially the physics associated with Ri-dependent mixing—release of mean kinetic energy working against stability. A large component of the energy spectrum in such models is derived from surface forcing—the boundary condition on the last term of (12). As a result, they also tend to operate to parameterize surface mixing (Kantha and Clayson 1994). [Recent studies by Blanke and Delecluse (1993) and Smith and Hess (1993) examined behavior of trop-

ical level-coordinate OGCMs using both the Pacanowski and Philander (1981) scheme and turbulence closure models, and may be consulted for their similarities and differences from other aspects.]

We would also note that in the study of Rosati and Miyakoda (1988), a comparison was made in model results between a case with the Mellor and Yamada (1982) level 2.5 turbulent closure model and an ''A'' physics that had a constant viscosity. A substantial improvement in the equatorial undercurrent at 95°W was reported. It should be considered, however, that the ''A'' physics had a constant viscosity of 30×10^{-4} m^2 s^{-1}, which is equivalent to the case reported in the top panels of Fig. 6 that completely failed to reproduce the annual cycle of the undercurrent. We therefore question whether the turbulence closure model provides any significant improvement over what could have been obtained by substantially reducing the background mixing.

Acknowledgments. This work was supported by NASA RTOP 578-41-45-78 and by the NOAA TOGA Program on Prediction. Discussions with Dake Chen, Pascale Delecluse, Ed Harrison, Bohua Huang, Jay McCreary, Mike McPhaden, Dennis Moore, and Hartmut Peters were useful. Suggestions by the anonymous reviewers helped to improve the manuscript. The services of the NASA Center for Computer Sciences were invaluable in accomplishing the large volume of computations necessary for this study.

REFERENCES

Blanke, B., and P. Delecluse, 1993: Variability of the tropical Atlantic Ocean simulated by a general circulation model with two different mixed-layer physics. *J. Phys. Oceanogr.*, **23,** 1363–1388.

Bleck, R., and D. Boudra, 1986: Wind-driven spin-up in eddy-resolving ocean models formulated in isopycnic and isobaric coordinates. *J. Geophys. Res.*, **91,** 7611–7621.

Chen, D., L. M. Rothstein, and A. J. Busalacchi, 1994: A hybrid vertical mixing scheme and its application to tropical ocean models. *J. Phys. Oceanogr.*, **24,** 2156–2179.

Gargett, A. E., and G. Holloway, 1984: Dissipation and diffusion by internal wave breaking. *J. Mar. Res.*, **42,** 15–27.

Gent, P. R., 1991: The heat budget of the TOGA-COARE domain in an ocean model. *J. Geophys. Res.*, **96,** 3323–3330.

——, and M. A. Cane, 1988: A reduced gravity, primitive equation model of the upper equatorial ocean. *J. Comput. Phys.*, **81,** 444–480.

Haney, R. L., 1971: Surface thermal boundary condition for ocean circulation models. *J. Phys. Oceanogr.*, **1,** 214–248.

Harrison, D. E., 1989: On climatological monthly mean wind stress and wind stress curl fields over the World Ocean. *J. Climate*, **2,** 57–79.

Hazel, P., 1972: Numerical studies of the stability of inviscid stratified shear flows. *J. Fluid Mech.*, **51,** 39–61.

Hellerman, S., and M. Rosenstein, 1983: Normal monthly wind stress over the World Ocean with error estimates. *J. Phys. Oceanogr.*, **13,** 1093–1104.

Howard, L., 1961: Note on a paper of John W. Miles. *J. Fluid Mech.*, **10,** 509–512.

Jones, J. H., 1973: Vertical mixing in the Equatorial Undercurrent. *J. Phys. Oceanogr.*, **3,** 286–296.

Kantha, L. H., and C. A. Clayson, 1994: An improved mixed layer model for geophysical applications. *J. Geophys. Res.*, **99,** 25 235–25 266.

Kraus, E. B., Ed., 1977: *Modelling and Prediction of the Upper Layers of the Ocean.* Pergamon, 325 pp.

——, 1990: Diapycnal mixing. *Climate–Ocean Interaction,* M. E. Schlesinger, Ed., Kluwer, 269–194.

——, and J. S. Turner, 1967: A one-dimensional model of the seasonal thermocline: II. The general theory and its consequences. *Tellus*, **19,** 98–106.

Large, W., J. C. McWilliams, and S. C. Doney, 1994: Oceanic vertical mixing: A review and a model with a nonlocal boundary layer parameterization. *Rev. Geophys.*, **32** (4), 363–403.

Levitus, S., 1982: *Climatological Atlas of the World Ocean.* NOAA Professional Paper No. 13, U. S. Govt. Printing Office, 173 pp. and 17 microfiche

McPhaden, M. J., and M. McCarty, 1992: Mean seasonal cycles and interannual variations at 0°, 110° W and 0°, 140° W during 1980–1991. NOAA Tech. Memo. ERL PMEL-95, 118 pp. [Available from NOAA/PMEL/OCRD, 7600 Sand Point Way, NE, Seattle, WA 98115.]

Mellor, G. L., and T. Yamada, 1974: A hierarchy of turbulence closure models for planetary boundary layers. *J. Atmos. Sci.*, **31,** 1791–1806.

——, and P. A. Durbin, 1975: The structure and dynamics of the ocean surface mixed layer. *J. Phys. Oceanogr.*, **5,** 718–728.

——, and T. Yamada, 1982: Development of turbulence closure models for geophysical fluid problems. *Rev. Geophys.*, **20,** 851–875.

Miles, J., 1961: On the stability of heterogeneous shear flows. *J. Fluid Mech.*, **10,** 496–508.

Moum, J., and T. R. Osborn, 1986: Mixing in the main thermocline. *J. Phys. Oceanogr.*, **16,** 1250–1259.

——, D. R. Caldwell, and C. A. Paulson, 1989: Mixing in the equatorial surface layer and thermocline. *J. Geophys. Res.*, **94,** 2005–2021.

Murtugudde, R., M. A. Cane, and V. Prasad, 1995: A reduced-gravity, primitive equation, isopycnal ocean GCM: Formulation and simulations. *Mon. Wea. Rev.*, **123,** 2865–2887.

Niiler, P. P., and E. B. Kraus, 1977: One-dimensional models of the upper ocean. *Modelling and Prediction of the Upper Layers of the Ocean,* E. B. Kraus, Ed., Pergamon, 143–172.

Oberhuber, J., 1993: Simulation of the Atlantic circulation with a coupled sea ice–mixed layer–isopycnal general circulation model. Part I: Model description. *J. Phys. Oceanogr.*, **23,** 808–829.

Pacanowski, R., and S. G. H. Philander, 1981: Parameterization of vertical mixing in numerical models of tropical oceans. *J. Phys. Oceanogr.*, **11,** 1443–1451.

Peters, H., M. C. Gregg, and J. M. Toole, 1988: On the parameterization of equatorial turbulence. *J. Geophys. Res.*, **93,** 1199–1218.

Price, J. F., R. A. Weller, and R. Pinkel, 1986: Diurnal cycling: Observations and models of the upper ocean response to diurnal heating, cooling, and wind mixing. *J. Geophys. Res.*, **91,** 8411–8427.

Qiao, L., and R. H. Weisberg, 1997: The zonal momentum balance of the Equatorial Undercurrent in the central Pacific. *J. Phys. Oceanogr.* **27,** 1094–1119.

Reynolds, R. W., 1982: A monthly averaged climatology of sea surface temperatures. NOAA Tech. Rep. NWS31, 35 pp. [Available from NOAA/NWS/NCEP, 5200 Auth Road, Camp Springs, MD 20746.]

Robinson, A., 1966: An investigation into the wind as the cause of the Equatorial Undercurrent *J. Mar. Res.*, **24,** 179–204.

Rosati, A., and K. Miyakoda, 1988: A general circulation model for upper ocean simulation. *J. Phys. Oceanogr.*, **18,** 1601–1626.

Schopf, P. S., and A. Loughe, 1995: A reduced gravity isopycnal ocean model: Hindcasts of El Niño. *Mon. Wea. Rev.*, **123,** 2839–2863.

Shapiro, R., 1970: Smoothing, filtering and boundary effects. *Rev. Geophys. Space Phys.*, **8,** 359–387.

Smith, N. R., and G. D. Hess, 1993: A comparison of vertical eddy mixing parameterizations in equatorial ocean models. *J. Phys. Oceanogr.*, **23,** 1823–1830.

Thorpe, S., 1973: Experiments on instability and turbulence in a stratified shear flow. *J. Fluid Mech.*, **61,** 731–751.